Improved variational many-body wave function in light nuclei

Q. N. Usmani,[1,*] A. Singh,[2] K. Anwar,[1] and G. Rawitscher[3]
[1]*Institute of Engineering Mathematics, University Malaysia Perlis, Malaysia*
[2]*Department of Physics, School of Technology, Kalinga Institute of Industrial Technology, Bhubaneswar 751 024, India*
[3]*Department of Physics, University of Connecticut, Storrs, Connecticut 06269-3046, USA*
(Received 29 May 2009; published 10 September 2009)

We propose and implement a simple method for improving the variational wave function of a many-body system. We have obtained a significant improvement in the binding energies, wave functions, and variance for the light nuclei ^{3}H, ^{4}He, and ^{6}Li, using the fully realistic Argonne (AV_{18}) two-body and Urbana-IX (UIX) three-body interactions. The energy of ^{4}He was improved by about 0.2 MeV and the ^{6}Li binding energy was increased by $\approx$1.7 MeV compared to earlier variational Monte Carlo results. The latter result demonstrates the significant progress achieved by our method, and detailed analyses of the improved results are given. With central interactions the results are found to be in agreement with the "exact" calculations. Our study shows that the relative error in the many-body wave functions, compared to two-body pair correlations, increases rapidly at least proportionally to the number of pairs in the system. However, this error does not increase indefinitely since the pair interactions saturate owing to convergence of cluster expansion.

DOI: 10.1103/PhysRevC.80.034309 PACS number(s): 21.60.Ka, 13.75.Cs, 21.10.Dr, 27.10.+h

I. INTRODUCTION

The variational Monte Carlo (VMC) method has wide applications and is an established powerful tool in the areas of nuclear [1–11], molecular, and condensed matter [12] physics. In nuclear physics, its importance can be gauged by its relevance to a large number of calculations. In addition to calculating energies and other properties of nuclei, it has been employed to calculate the electromagnetic elastic and transition form factors in ^{6}Li [1], to calculate spectroscopic factors in the ^{7}Li$(e,e'p)$ reaction [2], to calculate spectroscopic amplitudes used as input to the distorted-wave Borm approximation (DWBA) analysis of radioactive beam experiments [3], and in astrophysical radiative capture reactions such as $d(\alpha,\gamma)^6$Li, $t(\alpha,\gamma)^7$Li, and ^{3}He$(\alpha,\gamma)^7$Be [4]. It has also been used in a number of calculations in hypernuclei [5,6]. Equally important is that it is used as a starting trial wave function, where its quality is crucial, for Green's function Monte Carlo (GFMC) calculations [7–11]. The VMC method produces good results for few-body systems when the constituent particles interact with simple interactions. However, with complicated interactions, the method gives only approximate solutions for few-body systems and in addition the results deteriorate rapidly as the number of particles increases in the system [8,10]. In this paper, we propose and implement a technique to improve upon the variational wave functions for a many-body system where the constituent particles interact through complicated interactions. First we analyze the effect of the errors as a function of the number of particles in the variational wave function and then correct them in a suitable manner. We consider nuclear many-body systems, where the nucleons interact through two-body AV_{18} [13] and UIX [14] three-body interactions. These interactions are extremely complicated in nature with complex operatorial dependence. The improved method is applied to the pair correlation functions as well as to each pairwise link of the three-body correlations of the total wave function for ^{3}H, ^{4}He, and ^{6}Li. The present results from the improved method account for significant differences between the GFMC [8] and the earlier VMC calculations. We also perform calculations with central interactions (Minnesota [15] and Malfliet-Tjon V [16]) for ^{3}H, ^{4}He, and ^{6}Li as well as ^{6}He. Results for these are in complete agreement with precise variational solutions that use the stochastic variational method (SVM) [17]. It is hoped that the present study and its follow-up on the suggested lines shall be useful in calculations in light nuclei. We confine ourselves to the known nuclear correlations and their structures as proposed and developed by Pandharipande and collaborators [18–22]. For brevity, we shall write it as the PANDC Collaboration.

Usually, the variational wave function for a complicated interaction similar to AV_{18} is approximate on two counts. First, there are approximations in the radial shape of the functions; second, the correlation structures in themselves are not fully understood or known. In this paper, we shall be concerned with correcting the known approximate correlations. In a subsequent paper, new correlations shall be incorporated.

For VMC calculations in light nuclei with an interaction such as AV_{18}, the calculations proceed with f_8 correlations, which are obtained as solutions of eight two-body coupled differential equations. These contain a number of variational parameters that have been introduced over a number of years based upon physical and intuitive considerations. AV_{18} is also found to induce important three-body correlations in light nuclei [22]. Three-body interaction and p-shell nuclei add additional correlations whose shapes and structures are guided by perturbation theory and various features of the shell model. However, the radial shapes of these correlations are largely approximate.

In Sec. II, we demonstrate that, as the number of particles in the system increases, the relative error in the wave function increases at least in proportion to the number of particle pairs.

*qnusmani@hotmail.com

This makes the many-body wave function more approximate as the number of particles increases in the system. A simple method is devised that corrects these errors variationally. In Sec. III, we describe the wave function for light nuclei and the correction required to improve upon the wave function. In Sec. IV we present our results for central as well as for the AV_{18} + UIX interactions. Conclusions are presented in Sec. V.

II. ERROR ANALYSIS

We first consider the case of Jastrow correlations. The wave function is written as a product of two-particle correlation functions. If $\varepsilon(r)$ represents the as-yet unknown variational error in each correlation function, we have

$$\Psi^a = \prod_{i<j} f^a_{ij} = \prod_{i<j} (f_{ij} + \varepsilon_{ij}), \tag{2.1}$$

where f^a_{ij} and f_{ij} represent, respectively, the approximate and the desired correlation functions and Ψ^a is the approximate total wave function. f^a_{ij} is usually obtained through the solution of a Schrödinger-type two-body equation containing variational parameters through a suitably modified NN potential for variational purposes [8,18–22]. For the moment we disregard the antisymmetry and other components, namely, three-body and other correlations that may be present in the wave function. We include these in our calculations at a later stage.

Expression (2.1) can also be written as

$$\begin{aligned}\Psi^a &= \left(\prod_{i<j} f_{ij}\right)\left(\prod_{k<l}(1+\varepsilon_{kl}/f_{kl})\right)\\ &= \Psi\left(\prod_{k<l}(1+\varepsilon_{kl}/f_{kl})\right),\end{aligned} \tag{2.2}$$

where Ψ is the "exact" or desired variational wave function within the limitations just mentioned. For terms linear in ε the relative error in the wave function is

$$\frac{\Psi^a}{\Psi} = \prod_{k<l}(1+\varepsilon_{kl}/f_{kl}). \tag{2.3}$$

For a three- or four-particle system if the particles are located at the vertices of an equilateral triangle (three particles) or a regular tetrahedron (four particles), we have $\Psi^a/\Psi \approx 1 + n_p\varepsilon/f$, where n_p is the number of pairs. Thus the relative error in case of a many-particle system is enhanced by a factor that is proportional at least to n_p as compared to the errors in a two-particle system. Errors in the variational energies will then be proportional to n_p^2. It is important to note that, in view of the presence of the functions f_{kl} in the denominator, the errors are amplified wherever f_{kl} are small. This will occur for low values of r for repulsive potentials at short distances and in the asymptotic regions for finite bound systems. This can be clearly seen in Figs. 4 and 5 of Ref. [22]. However, these regions are sampled with much less probability because the wave functions for these configurations are small. It also follows that if ε is not small the relative errors will be proportional to the number of triplets and quartets etc., in addition to the number of pairs. We therefore arrive at the important conclusion that the relative error in the wave function increases rapidly as the number of particles increases in the system. This probably could be one of the reasons why VMC results deteriorate in the p-shell region with increasing mass number. For example, the VMC energies for ^{6}Li and ^{12}C are roughly higher by 3 and 30 MeV, respectively, compared to GFMC energies [8,10]. There can also be other reasons responsible for the deterioration in the energy with higher mass number. For example, addition of more particles may give rise to new correlations, which are not included in PANDC, or for higher mass numbers, optimization of PANDC correlations may become difficult. But this does not imply that for heavier nuclei or in the extreme case of nuclear matter the situation is hopeless. Fortunately, because of the saturating nature of the nuclear forces, as the number of particles in the system increases the number of effective correlated pairs remains finite (mostly the immediate neighbors correlate). For example, if one makes an *irreducible* cluster expansion of the wave function [23] the contribution to the energy of successive many-body cluster terms converges after a finite number of terms. Thus the errors in the correlations will also tend to saturate.

These considerations will also hold for operatorial and three-body correlations. On the basis of these arguments, we may expect that improvement in the radial shape of correlations will affect the lowering of energies more in heavy nuclei, for example in ^{6}Li as compared to ^{3}H. These expectations are supported by actual calculations as demonstrated in this study.

We consider the following simple technique to improve upon the approximate variational wave function. We add to ε_{ij} in Eq. (2.1) a function γ_{ij}, which is determined variationally. This leads to

$$\varepsilon_{ij} - \gamma_{ij} \cong 0. \tag{2.4}$$

We determine the variational functions γ through the use of a convenient set of orthonormal polynomials L_m [5]:

$$\gamma(r) = \sum_{n=0}^{K} a_n L_n(r) \quad \text{for} \quad r \leqslant r_d, \tag{2.5}$$

where a_n are variational parameters. We also impose the condition that $\gamma(r)$ and at least its first derivative are zero at $r = r_d$, where r_d is the healing distance. The healing distance is also a variational parameter. We have used for $L_n(r)$ the function $\cos(n\pi r/r_d)$. In a few test cases, we have used the combination of $\cos(n\pi r/r_d)$ and $\sin(n\pi r/r_d)$ functions as well as the Chebyshev polynomials for $L_n(r)$ without any significant differences in the results. The function $\cos(n\pi r/r_d)$ has the advantage that its first derivative vanishes at $r = 0$ and r_d. Usually, a large value of K would be required to satisfy Eq. (2.4). For $L_n(r) = \cos(n\pi r/r_d)$, the condition that $\gamma(r) = 0$ at $r = r_d$ gives

$$a_0 = \sum_{n=1}^{K} (-1)^{n+1} a_n. \tag{2.6}$$

III. WAVE FUNCTION

The Minnesota (Minn.) potential has central, spin, isospin, and spin-isospin parts. As stated earlier we follow the wave function construct and techniques developed by the PANDC Collaboration for carrying out variational calculations in light nuclei. Corresponding to each component of the interaction the wave function consists of central (f_c), isospin (u_τ), spin (u_σ), and spin-isospin ($u_{\sigma\tau}$) correlations. The variational wave function for particles interacting through Minnesota or Malfeit-Tjon potentials mainly consists of these with some additional three-body correlations as explained later. Potentials such as $AV_{18} + UIX$ induce considerable complicated structure in the wave function. The state-of-the-art variational wave function of s- and p-shell nuclei is of the form

$$|\Psi_V\rangle = \left[1 + \sum_{i<j<k} \left(U_{ijk} + U_{ijk}^{TNI}\right) + \sum_{i<j} U_{ij}^{LS}\right] \times \left[S \prod_{i<j} (1 + U_{ij})\right] |\Psi_J\rangle\,, \tag{3.1}$$

where the various U's shall be explained a little later. The operator S symmetrizes the noncommuting product operators $(1 + U_{ij})$. The wave function [Eq. (3.1)] is explained in Ref. [8] and earlier Refs. [18–22], but here since we modify almost each and every component of these it is desirable that we discuss them in detail. For s-shell nuclei, the following Jastrow function $|\Psi_J\rangle$ is employed:

$$|\Psi_J\rangle = \left[\prod_{i<j<k} f_{ijk}^c(\vec{r}_{ij}, \vec{r}_{jk}, \vec{r}_{ki}) \prod_{i<j} f_c(r_{ij})\right] |\Phi_A\,(JMTT_3)\rangle. \tag{3.2}$$

The central two- and three-body correlations f_c and f_{ijk}^c have no spin or isospin dependence. Φ_A is an antisymmetrized spin-isospin state.

For light p-shell nuclei, shell-model studies [24] suggest that the LS coupling scheme is a good approximation for obtaining the desired JM values of a given state. The Jastrow function is more complicated owing to additional correlations specific to p-shell nucleons and the possibilities of different possible LS combinations, which lead to several components in the wave function. Allowing for the possibility that the central correlation f_c may assume different shapes for ss, sp, and pp nucleons, we may write

$$|\Psi_J\rangle = \left(\prod_{i<j<k} f_{ijk}^c \prod_{i<j\leqslant k} f_{ss}(r_{ij}) \prod_{k\leqslant 4<l\leqslant A} f_{sp}(r_{kl})\right) \times \left\{\sum_{LS[n]} \left(\beta_{LS[n]} \prod_{4<l<m\leqslant A} f_{pp}^{LS[n]}\,(r_{lm}) \times |\Phi_A\,(LS[n]JMTT_3)_{1234:56\cdots A}\rangle\right)\right\}, \tag{3.3}$$

where A operates upon the total wave function and ensures its antisymmetry. In reality, this is an antisymmetric sum of all possible partitions of four s-shells and the remaining $A - 4$ p-shell nucleons. The f_{sp} at short distances has the same behavior as f_{ss} (or f_c) but asymptotically goes to unity. This allows for the possibility that the wave function factorizes to a cluster formation similar to $\alpha + d$ in ^{6}Li. $\beta_{LS[n]}$ are variational parameters that give the weights to the various LS components of the single-particle wave functions. This also allows for the possibility that the two-nucleon correlations between two p-shell nucleons may assume different shapes for different LS components. The single-particle wave function for different LS components is given by

$$\begin{aligned}&|\Phi_A\,(LS[n]JMTT_3)_{1234:56\cdots A}\rangle \\ &= |\Phi_\alpha(0000)\rangle_{1234} \prod_{4<l\leqslant A} \phi_p^{LS[n]}(R_{\alpha l}) \left\{\left[\prod_{4<l\leqslant A} Y_{1m_l}(\Omega_{\alpha l})\right]_{LM_l[n]} \times \left[\prod_{4<l\leqslant A} \chi_l\left(\tfrac{1}{2}m_s\right)\right]_{SM_S}\right\}_{JM} \left[\prod_{4<l\leqslant A} \nu_l\left(\tfrac{1}{2}t_3\right)\right]_{TT_3},\end{aligned} \tag{3.4}$$

where Φ_α is an antisymmetrized spin-isospin state of the α particle. The $\phi_p^{LS[n]}(R_{\alpha k})$ are single-particle wave functions of a p-shell nucleon obtained by assuming that the nucleon is moving in an effective Woods-Saxon potential

$$V(R_{\alpha N}) = V_p^{LS}\left[1 + \exp\left(\frac{R_{\alpha N} - R_p}{a_p}\right)\right]^{-1}, \tag{3.5}$$

where $R_{\alpha N}$ is the relative distance between a p-shell nucleon and the center of mass of the α particle. The Woods-Saxon parameters ${V_p}^{LS}$, R_p, and a_p are treated as variational parameters and are different for different $LS[n]$ components.

The correlations f_{sp} and $f_{pp}^{LS[n]}$ are assumed to have the form

$$f_{sp}(r) = \frac{f_c(r)}{[1 + \exp(r - s_1)]} + s_2\{1 - \exp[-(r/s_3)^2]\}, \tag{3.6}$$

$$f_{pp}^{LS[n]} = f_c(r) + b_1^{LS[n]}\left\{1 - \exp\left[-\left(r/b_2^{LS[n]}\right)^2\right]\right\}, \tag{3.7}$$

where $s_{1\text{-}3}$ and $b_{1\text{-}2}^{LS[n]}$ are variational parameters. The parameters $s_{1\text{-}3}$ have been determined earlier with values of 4.0, 0.90, and 3.2, respectively [8,25]. In earlier studies by Wiringa and collaborators more general forms of f_{sp} and $f_{pp}^{LS[n]}$ have been employed. The different $LS[n]$ combinations for ^{6}Li are 01[2], 21[2], and 10[11]; for brevity we denote them as 1, 2, and 3, respectively, in ϕ_p(1–3) and f_{pp}(1–3).

In Eq. (3.1), the U_{ij} is a sum of noncommuting spin, isospin, and tensor operators:

$$U_{ij} = \sum_{p=2,6} \left[\prod_{k\neq i,j} f_{ijk}^p(\vec{r}_{ij}, \vec{r}_{jk}, \vec{r}_{ki})\right] u_p(r_{ij}) O_{ij}^p. \tag{3.8}$$

In general, the operators O_{ij}^p for AV_{18} are

$$O_{ij}^{p=1,14} = [1, \vec{\sigma}_i \cdot \vec{\sigma}_j, S_{ij}, \vec{L} \cdot \vec{S}, L^2, L^2(\vec{\sigma}_i \cdot \vec{\sigma}_j), (\vec{L} \cdot \vec{S})^2] \otimes [1, \vec{\tau}_i \cdot \vec{\tau}_j], \tag{3.9}$$

$$O_{ij}^{p=15,18} = [1, \vec{\sigma}_i \cdot \vec{\sigma}_j, S_{ij}] \otimes T_{ij} \text{ and } (\vec{\tau}_{zi} + \vec{\tau}_{zj}), \tag{3.10}$$

where $T_{ij} = 3\tau_{zi}\tau_{zj} - \vec{\tau}_i \cdot \vec{\tau}_j$ is the isotensor operator. All the symbols have their usual meanings.

In Eq. (3.8), the sum over p is from 2 to 6; that is,

$$O_{ij}^{p=2,6} = \vec{\tau}_i \cdot \vec{\tau}_j, \vec{\sigma}_i \cdot \vec{\sigma}_j, (\vec{\sigma}_i \cdot \vec{\sigma}_j)(\vec{\tau}_i \cdot \vec{\tau}_j), S_{ij}, S_{ij}(\vec{\sigma}_i \cdot \vec{\sigma}_j)(\vec{\tau}_i \cdot \vec{\tau}_j). \tag{3.11}$$

These are abbreviated as τ, σ, $\sigma\tau$, t, and $t\tau$ and the corresponding u's are denoted as u_τ, u_σ,$u_{\sigma\tau}$, u_t, and $u_{t\tau}$, respectively. The U_{ij}^{LS} in Eq. (3.1) are given by

$$U_{ij}^{LS} = \sum_{p=7,8} \left[\prod_{k\neq i,j} f_{ijk}^{p}(\vec{r}_{ij}, \vec{r}_{jk}, \vec{r}_{ki}) \right] u_p(r_{ij}) O_{ij}^{p}, \tag{3.12}$$

with

$$O_{ij}^{p=7,8} = \vec{L}.\vec{S} \quad \text{and} \quad \vec{L}.\vec{S}\left(\vec{\tau}_i \cdot \vec{\tau}_j\right). \tag{3.13}$$

The corresponding u's are denoted as u_b and $u_{b\tau}$, respectively. The eight u's are obtained by minimizing the two-body cluster energy with a somewhat modified two-nucleon interaction. Specifically, this modification comes through the use of quenched interactions and parametrized Lagrange multipliers to lower the many-body variational energy. The Lagrange multipliers also take care of the asymptotic boundary conditions on the wave function for the appropriate single-particle separable behavior at large distances. The quenched interaction $\bar{v}$ is related to the bare interaction by

$$\bar{v}_{ij} = \sum_{p=1}^{n} \alpha_p v_p(r_{ij}), \tag{3.14}$$

where α_p are variational parameters. The Lagrange multipliers $\lambda_p(r)$ are radial functions, consisting of two parts. The short-range part simulates the screening effect and the long-range part is fixed by the asymptotic behavior of the correlation functions, which is cut off at short distances by an exponential function:

$$\lambda_p(r) = \Gamma_p \left[1 + \exp\left(\frac{r - R_p}{a_p} \right) \right]^{-1} + \Lambda_p(r,\kappa_x)[1 - \exp(-(r/c_p)^2)]. \tag{3.15}$$

The constant (eigenvalue) Γ_p is determined by solving the Schrödinger-type differential equation subject to boundary conditions on the wave function [21]. The parameters R_p, a_p, c_p, and κ_x (explained in the following) are variational parameters.

The eight correlation functions f_c and $u_{p=2\text{-}8}$ can be expressed in terms of central functions $f_{S,T}$ (r) $(T = 0,1;$ $S = 0,1)$, tensor functions $f_{t,T}(r)$, and spin-orbit functions $f_{b,T}(r)$ [21]. The boundary conditions on these for $r \to \infty$ are

$$f_{S,T}(r \to \infty) = \left[\frac{\exp(-\kappa_{S,T} r)}{r} \right]^{\frac{1}{A-1}}, \tag{3.16a}$$

$$f_{t,T}(r \to \infty) = \eta_T T(r) f_{S,T}(r), \tag{3.16b}$$

$$f_{b,T}(r \to \infty) = \varsigma_T B(r) f_{S,T}(r), \tag{3.16c}$$

where

$$T(r) = \left[1 + \frac{3}{\kappa_{S,T} r} + \frac{3}{(\kappa_{S,T} r)^2} \right] \{1 - \exp[-(r/d_{t,T})^2]\},$$
$$B(r) = \left[\frac{1}{r^2} + \frac{\kappa_{S,T}}{r} \right] \{1 - \exp[-(r/d_{b,T})^2]\}, \tag{3.17}$$
$$\kappa_{S,T} = \left[\frac{A-1}{A} \frac{2m}{\hbar^2} E_{S,T} \right]^{\frac{1}{2}}.$$

The tensor/central ratio η_T, the spin-orbit/central ratio ζ_T, and the separation energies $E_{S,T}$ are variational parameters.

All the variational parameters are determined by minimizing the expectation values of the energy using the Metropolis random walk method [8,21]. We mainly employ the same values of the variational parameters as in Refs. [8,21], but now we introduce additional variational parameters by modifying f_c and the seven u's by substituting

$$f_c \to f_c + \sum_{n=0}^{K} a_n^c \cos\left(n\pi r / r_d^c\right),$$
$$u_p \to u_p + \sum_{n=0}^{K} a_n^p \cos\left(n\pi r / r_d^p\right) \tag{3.18}$$

for p = 2–8. Similarly, we modify f_{sp}, $f_{pp}^{LS[n]}$, and $\phi_p^{LS[n]}$; the corresponding variational parameters are denoted as a_n^{sp}, $a_n^{pp}(LS[n])$, and $a_n^p(LS[n])$, respectively. The values of K may be different for different interactions. For interactions such as Malfliet-Tjon, which is singularly repulsive near the origin, larger values of K were required. Also, the value of K may be larger if the initial correlations f_c or u_p are not properly optimized. In addition, the values of K may be different for different correlations. Modifications similar to Eq. (3.16) are employed for three-body correlations also. However, the same value of K has been used for all the correlations for a given nucleus.

The three-body correlations f_{ijk}^c, f_{ijk}^p, and U_{ijk} are induced by the two-nucleon interaction [22]. For f_{ijk}^c and f_{ijk}^p, the following forms have been employed:

$$f_{ijk}^c = 1 + q_1^c (r_{ij} \cdot r_{ik})(r_{ji} \cdot r_{jk})(r_{ki} \cdot r_{kj}) \exp\left(-q_2^c R_{ijk}\right), \tag{3.19}$$

$$f_{ijk}^p = 1 - q_1^p (1 - \hat{r}_{ij} \cdot \hat{r}_{jk}) \exp\left(-q_2^p R_{ijk}\right), \tag{3.20}$$

with $R_{ijk} = r_{ij} + r_{jk} + r_{ki}$. The various q's are the variational parameters. In f_{ijk}^c we do allow the possibility that $q_{1\text{-}2}^c$ may be different if the ijk refer to nucleons in different shells. Thus for ^{6}Li we may have three sets of $q_{1\text{-}2}^c(sss)$, $q_{1\text{-}2}^c(ssp)$, and $q_{1\text{-}2}^c(spp)$, where s and p refer to s- and p-shell nucleons. The U_{ijk} correlations consist of a spin orbit and an isospin component. The spin-orbit part is given by

$$U_{ijk}^{ls} = \sum_{cyc} i\vec{\sigma}_i \cdot (\vec{r}_{ij} \times \vec{r}_{ik})[g_{ik}(h_{ij} - h_{jk}) - g_{ij}(h_{ik} - h_{jk})], \tag{3.21}$$

where

$$h(r) = q_1^{ls} \exp\left(-q_2^{ls} r^2\right) + \sum_{n=0}^{K} a_n^h \cos\left(n\pi r_{ij} / r_d^h\right) \tag{3.22}$$

and

$$g(r) = \exp\left(q_3^{ls} r^2\right) + \sum_{n=0}^{K} a_n^g \cos\left(n\pi r_{ij} big / r_d^g\right). \quad (3.23)$$

The isospin component is given by

$$U_{ijk}^{\tau} = \sum_{cyc} \left(\tfrac{1}{3} R_{ijk} - r_{ij}\right) \left\{q_1^{\tau} \exp\left[-q_2^{\tau}\left(X_{ijk} - q_3^{\tau}\right)^2\right] - 2q_1^{\tau} \exp\left(-2q_2^{\tau} X_{ijk}^2\right)\right\} \vec{\tau}_i \cdot \vec{\tau}_j, \quad (3.24)$$

where

$$X_{ijk} = \left[1 + q_4^{\tau}(\hat{r}_{ij} \cdot \hat{r}_{ik})(\hat{r}_{ji} \cdot \hat{r}_{jk})(\hat{r}_{ki} \cdot \hat{r}_{kj})\right] R_{ijk}. \quad (3.25)$$

All seven q's in Eqs. (3.17)–(3.23) are variational parameters.

The three-body correlation U_{ijk}^{TNI} is induced by the three-nucleon interaction. It has two components:

$$U_{ijk}^{\mathrm{TNI}} = U_{ijk}^{\mathrm{FM}} + U_{ijk}^{R}, \quad (3.26)$$

where U_{ijk}^{FM} is the two-pion-exchange part of the correlation similar to the Fujita and Miyazawa [26] three-nucleon interaction. This is of the form

$$U_{ijk}^{\mathrm{FM}} = \sum_{cyc} \left(\delta_1 A_{2\pi} \{\vec{\tau}_i \cdot \vec{\tau}_j, \vec{\tau}_i \cdot \vec{\tau}_k\} \left\{X_{ij}^a, X_{ik}^a\right\} + \delta_2 C_{2\pi} [\vec{\tau}_i \cdot \vec{\tau}_j, \vec{\tau}_i \cdot \vec{\tau}_k] \left[X_{ij}^c, X_{ik}^c\right]\right). \quad (3.27)$$

The symbols a and c signify, respectively, that whether X occurs in the anticommutator, $\{\ \}$, or the commutator, $[\ ]$, terms. For Urbana IX, $A_{2\pi} = -0.02930$ MeV and $C_{2\pi} = A_{2\pi}/4$ MeV. δ_1 and δ_2 are variational parameters. The term $X_{ij}^{a(c)}$ stands for the operator

$$X_{ij}^{a(c)} = \left[T_{\pi}(r_s r_{ij}) + \sum_{n=0}^{K} a_n^{a(c)T} \cos\left(n\pi r_{ij} / r_d^{a(c)T}\right)\right] S_{ij} + \left[Y_{\pi}(r_s r_{ij}) + \sum_{n=0}^{K} a_n^{a(c)Y} \cos\left(n\pi r_{ij} / r_d^{a(c)Y}\right)\right] \vec{\sigma}_i \cdot \vec{\sigma}_j, \quad (3.28)$$

where r_s is a variational parameter. T_{π} and Y_{π} are the radial functions associated with the tensor and Yukawa parts of the one-pion-exchange potential:

$$T_{\pi}(r) = \left(1 + \frac{3}{\mu r} + \frac{3}{(\mu r)^2}\right) \frac{\exp(-\mu r)}{\mu r} [1 - \exp(-cr^2)]^2, \quad (3.29)$$

$$Y_{\pi}(r) = \frac{\exp(-\mu r)}{\mu r} [1 - \exp(-cr^2)], \quad (3.30)$$

with $\mu = 0.7$ fm^{-1} and the cutoff parameter $c = 2.1$ fm^{-2}.

For the U_{ijk}^{R}, we write

$$U_{ijk}^{R} = \delta_3 U_0 \sum_{cyc} \left[T_{\pi}^2(r_s r_{ij}) + \sum_{n=0}^{K} a_n^R \cos\left(n\pi r_{ij} / r_d^R\right)\right] \times \left[T_{\pi}^2(r_s r_{jk}) + \sum_{n=0}^{K} a_n^R \cos\left(n\pi r_{jk} / r_d^R\right)\right]. \quad (3.31)$$

$U_0 = 0.0048$ MeV for Urbana IX. δ_3 is a variational parameter. The modification in the radial shape of the three-body correlations is achieved through the variational parameters a_n^h, a_n^g, $a_n^{a(c)T(Y)}$, a_n^R, and r_d^x, where x stands for the corresponding superscripts in a_n. For all the $a_n = 0$ in Eqs. (3.28) and (3.31) and $\delta_1 = \delta_2 = \delta_3 = r_s = 1$, Eq. (3.24) reduces to the Urbana IX three-body interaction.

IV. RESULTS AND DISCUSSION

A. Central interactions

We first present our results for the central interactions (i.e., for Minnesota and Malfliet-Tjon V potentials). These are model calculations adopting different central potentials for which accurate or "exact" calculations have been performed earlier [17]. The results are summarized in Table I and compared with the SVM results of Ref. [17]. For the Minnesota potential calculations were performed for ^{3}H, ^{4}He, and ^{6}Li. They are in complete agreement with the SVM calculations of Ref. [17]. The Minnesota potential reproduces the important low-energy NN scattering data. In operator form it can be written as

$$V_{NN}(r_{ij}) = \sum_{p=1}^{4} v_p O_{ij}^p. \quad (4.1)$$

It therefore generates f_c, u_{τ}, u_{σ}, and $u_{\sigma\tau}$ correlations. This requires solution of four coupled Schrödinger-type equations to determine f_4. To demonstrate the power of our proposed technique we take a slightly different route. For the present case, instead of solving the f_4 coupled equations, f_c is obtained

TABLE I. Energies and rms radii of various nuclei calculated using the Minnesota and Malfleit-Tjon V potentials and compared with the SVM calculations. K is the dimension of the basis functions used in the SVM and present VMC calculations.

Nucleus	Interaction	SVM			VMC		
		K	E (MeV)	rms (fm)	K	K (MeV)	rms (fm)
^{3}H	Minn.	40	−8.38	1.698	7	−8.38(1)	1.709(3)
^{4}He	Minn.	60	−29.937	1.41	7	−29.940(4)	1.409(1)
^{6}Li	Minn.	600	−34.59	2.22	7	−34.59(1)	2.170(2)
^{6}He	MTV	800	−66.30	1.52	19	−67.15(2)	1.537(1)

by solving the Schrödinger-type equation with the central part of the potential only. This is then modified variationally by using the first relation of Eqs. (3.16). The three u_p are obtained by using directly the relation

$$u_p = \sum_{n=0}^{K} a_n^p \cos\left(n\pi r/r_d^p\right). \tag{4.2}$$

For ^{6}Li, correlations specific to the p-shell are obtained as described in the previous section. We use $\hbar^2/m = 41.47$ MeV fm^2. The Coulomb interaction is included with the Minnesota potential by assuming a point charge with $e^2 = 1.44$ MeV fm. The Minnesota potential has a super soft core. It therefore generates very smooth correlations. Thus $K = 7$ was found more than sufficient to achieve the variational convergence of energies. An automated search for the variational parameters, namely a_n^p, and for ^{6}Li a_n^{sp}, $a_n^{pp}(LS[n])$, and $a_n^p(LS[n])$, was employed. None of the three-body correlations were needed for central potentials.

Because of the flexible nature of the correlations, in a straightforward minimization of the energy with a finite set of Monte Carlo configurations, the energy invariably goes to very low values with large error bars. This in fact raises the true expectation value of the energy. It therefore becomes essential to minimize a suitable combination of energy and variance or standard deviation σ defined as

$$\sigma = \left[\frac{\langle H^2\rangle - \langle H\rangle^2}{N-1}\right]^{1/2}, \tag{4.3}$$

where N is the number of statistically independent samples. We have minimized the function

$$\chi = |E + C| + m_p(N-1)^{1/2}\sigma, \tag{4.4}$$

where E is the expectation value of energy with the variational wave function described in Sec. III and C is a positive constant much larger than $|E|$. The mixing parameter m_p is chosen through trial and is different for different system. Larger values of m_p were used for small N and vice versa. Though there are clever methods available to minimize the VMC energy [12] with smaller N, we have not implemented these in the present study.

The case of ^{6}He with the MTV potential

$$V_{\rm MTV}(r) = 1458.05\exp(-3.11r)/r - 578.09\exp(-1.55r)/r \tag{4.5}$$

is somewhat conspicuous. Our result $-67.15(2)$ MeV for the energy is significantly lower than the SVM value of -66.30 MeV of Ref. [17]. These values are obtained without the Coulomb energy in the Hamiltonian. When we add the Coulomb energy contribution, our value then becomes $-66.30(2)$ MeV, in agreement with Ref. [17].

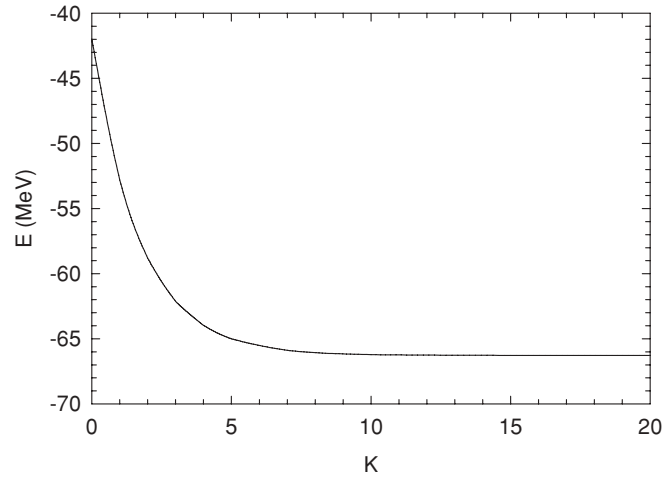

FIG. 1. Convergence of ^{6}He energy as a function of K with the Malfliet-Tjon V potential.

For the MTV potential a large value of K (=19) was needed. Figure 1 shows the convergence of E as a function of K. The reason for this convergence is that we started with a nonoptimized Jastrow wave function, where for $K = 0$, $E \approx -42.6(1)$ MeV. Except perhaps for the Coulomb energy discrepancy in ^{6}He the results are in excellent agreement with the SVM calculations of Ref. [17].

B. Argonne AV_{18} + UIX

With this interaction, we have studied ^{3}H, ^{4}He, and ^{6}Li. Calculations for ^{4}He and ^{6}Li were carried out on a modest four-node cluster whereas for ^{3}H a single-processor machine was used. Calculations were performed for two values of K, namely, 7 and 11. For ^{3}H and ^{4}He, $K = 7$ was found sufficient. No statistically significant improvements in results were found for $K = 11$. For ^{6}Li a lowering in the energy by 0.14 MeV was obtained between $K = 7$ and 11. The results are summarized in Table II. The entries for $K = 0$ correspond to VMC calculations without the modifications described in the previous section. These values are slightly different from the earlier VMC calculations mainly because of the use of slightly different variational parameters. Also the differences, though statistically insignificant, may arise because we have used a five-point (instead of a three-point) Lagrange interpolation formula for the various correlations tabulated on the fixed grid. Use of different seed values in

TABLE II. Variational energies and rms radii of various nuclei with the AV_{18} + UIX potential. The asterisk (*) value is for AV_{18} + IL2 [7].

Nucleus	Experiment		GFMC		VMC ($K = 0$)		K	VMC (present)	
	E (MeV)	$\langle r_p^2\rangle^{1/2}$	E (MeV)	$\langle r_p^2\rangle^{1/2}$	E (MeV)	$\langle r_p^2\rangle^{1/2}$		E (MeV)	$\langle r_p^2\rangle^{1/2}$
^{3}H	-8.482	1.60	$-8.46(1)$	1.59(0)*	$-8.32(1)$	1.58(0)	8	$-8.35(1)$	1.58(0)
^{4}He	-28.30	1.48(1)	$-28.34(4)$	1.45(1)	$-27.72(4)$	1.47(0)	8	$-27.90(2)$	1.44(0)
^{6}Li	-31.99	2.43(4)	$-31.15(11)$	2.57(1)	$-27.99(4)$	2.48(0)	12	$-29.69(3)$	2.58(0)

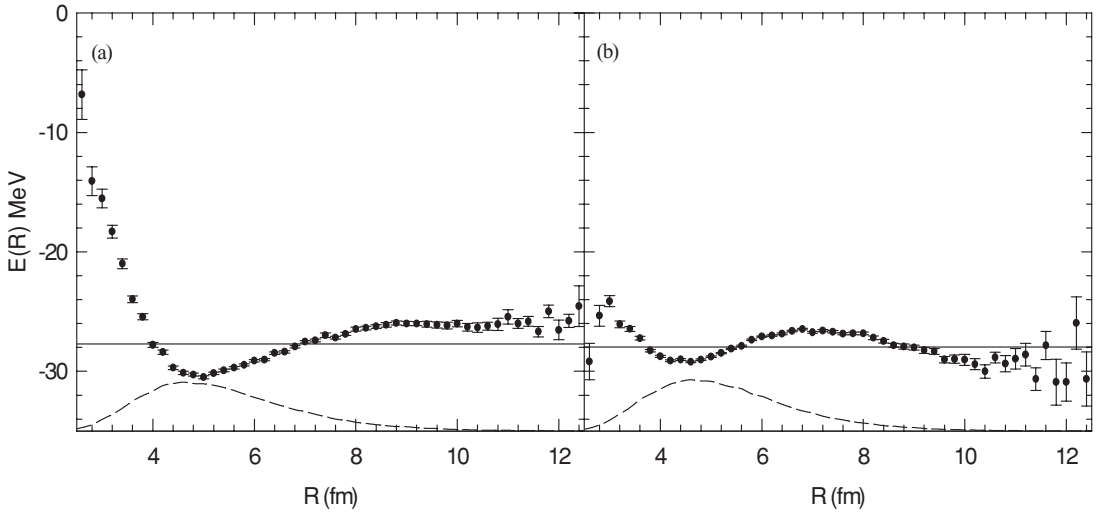

FIG. 2. Local energies for ^{4}He as a function of R. For details, see text.

generating the pseudorandom numbers may also account for some of the differences, but these are not important. The small differences between the present calculations with $K = 0$ and the earlier VMC calculations are not important as any deficiencies in the former compared to the latter is taken care of by the improvements in the variational wave function as demonstrated in Sec. IV A for ^{6}He with the MTV potential. Calculations for all the nuclei were performed for 100 000 random configurations. For s-shell nuclei, random walks were generated by including the full three-body correlations but dropping the U_{ij}^{LS} terms in Eq. (3.1). For ^{6}Li, only the U_{ijk} part of the three-body correlation was included.

In reference to Table II, we make the following observations. First, as the number of nucleons increases in the system the improvement in the energy also increases. For example, in ^{3}H the VMC energy for $K = 0$ is $-8.32(1)$ MeV, which becomes $-8.35(1)$ MeV, a small decrease of 0.03 MeV but statistically significant, whereas for ^{6}Li the decrease in energy is quite significant ($\approx$1.7 MeV). For ^{4}He, this decrease lies in between these two values (i.e., $\approx$0.18 MeV). This is in line with the qualitative arguments given in Sec. II, that as the number of particles increases in the system the relative error in the wave function increases proportionally at least to the number of pairs. This error then leads to a higher variational energy. Second, we notice a reduction in the variance. For all three nuclei a considerable reduction in the variance was obtained. The variance decreased to 0.0079 from 0.0147 for ^{3}H, to 0.0198 from 0.0407 for ^{4}He, and to 0.0273 from 0.0351 for ^{6}Li. This reduction indicates that there is an overall improvement in the wave function. We could obtain somewhat lower energies for smaller m_p in Eq. (4.4) but with a larger variance. We prefer to keep the variance small in view of the better quality of the wave function. Lowering of variance is an indication for the improvement in the wave function. For example, for an exact wave function, the variance will be zero.

The overall improvement in the wave function can also be seen by looking at the local energies. Figures 2 and 3 show curves for ^{4}He and ^{6}Li, respectively. $E(R)$ is the local energy

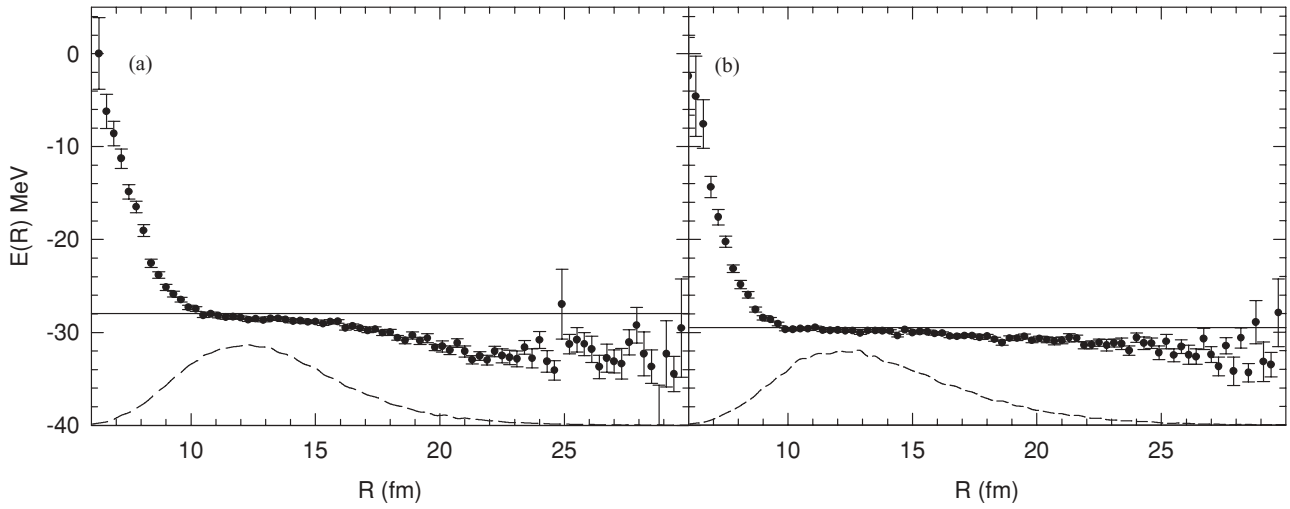

FIG. 3. Local energies for ^{6}Li as a function of R. For details, see text.

TABLE III. Two-body variational parameters. The superscripts a, b, c, d, and e refer to Eqs. (3.17), (3.16c), (3.16b), (3.15), and (3.14), respectively.

Nucleus	$E_{S,T}{}^a$	$\eta_T{}^b$	$\zeta_T{}^c$	$C_p{}^d$	$a_x{}^d$	$R_x{}^d$	$\alpha_p{}^e$
^{3}H	6.0	0.026	0.0	1.1	0.35	0.75	1.00
	3.2	−0.007	0.0003	1.1	0.35	0.75	0.91
	13.0			3.0	0.40	2.80	0.91
	6.4			3.0	0.40	2.80	0.91
				2.0	0.40	3.70	0.91
				2.0	0.40	3.70	0.91
				2.0	0.24	0.40	0.91
				2.0	0.24	0.40	0.91
^{4}He	16.0	0.035	0.0	1.1	0.35	0.75	1.00
	17.0	−0.015	0.0003	1.1	0.35	0.75	0.86
	23.5			3.0	0.40	2.80	0.86
	16.5			3.0	0.40	2.80	0.86
				2.0	0.40	3.70	0.86
				2.0	0.40	3.70	0.86
				2.1	0.24	0.40	0.86
				2.1	0.24	0.40	0.86
^{6}Li	16.0	0.035	0.0	1.1	0.35	0.75	1.00
	17.0	−0.015	0.0003	1.1	0.35	0.75	1.00
	23.5			3.0	0.40	2.80	1.00
	16.5			3.0	0.40	2.80	1.00
				2.0	0.40	3.70	0.86
				2.0	0.40	3.70	0.86
				2.0	0.24	0.40	1.10
				2.0	0.24	0.40	1.10

for a given spatial configuration $\mathbf{R} = (\mathbf{r}_1, \ldots, \mathbf{r}_4$ or $\mathbf{r}_6)$ binned as a function of the sum $R = \Sigma_i |r_i|$ of particle distances from the center of mass. The variance is also binned accordingly. The solid line is the average energy. The lower dashed curves

TABLE V. Correlations specific to ^{6}Li for p-shell nucleons The superscripts a, b, and c refer to Eqs. (3.3), (3.5), and (3.7), respectively.

$LS[n]$	$\beta_{LS[n]}{}^a$	$V_p^{LS\,b}$	$R_p{}^b$	$a_p{}^b$	$b_1^{LS[n]\,c}$	$b_2^{LS[n]\,c}$
01[2]	0.981	−20.0	4.0	1.5	0.1	3.2
21[2]	0.158	−18.0	4.0	1.5	0.1	3.2
10[11]	0.113	−18.0	4.0	1.5	0.1	3.2

give the relative probability of R occurrences in arbitrary units for 100 000 configurations. Figures 2(a) and 2(b) correspond to $K = 0$ and to $K = 7$, respectively, for ^{4}He, and Figs. 3(a) and 3(b) correspond to $K = 0$ and $K = 11$, respectively, for ^{6}Li. It is evident that the improved local energies are closer to the solid curve compared to $K = 0$ for almost all the important regions of R. In Tables III, IV, and V we give the values of the variational parameters that have been used in the present study. Table V gives correlation parameters for p-shell nucleons specific to ^{6}Li. These correlation parameters were determined mostly by Wiringa and collaborators [25]. In Table IV, the row with the asterisk on ^{6}Li gives the three-body correlation parameters $\delta_{1\text{-}3}$ that were used when modifications to correlations were implemented. The reason for employing a different set of $\delta_{1\text{-}3}$ parameters was simply to demonstrate and check the proposed modification; the initial values of the PANDC parameters do not play an important role though it is desirable to use optimized values for better convergence. We obtain essentially the same results when we use the unasterisked parameters.

In Tables VI and VII we give values of the variational parameters a_n^x for ^{4}He and ^{6}Li, respectively, along with the healing distance r_n^x, where x stands for various different correlations. Theses values are given up to five significant digits. Truncating them at four to two significant digits changes the random walk and the energies may go slightly higher. The parameters a_0^x for various x are fixed from the condition of

TABLE IV. Three-body variational parameters. The superscripts a, b, c, d, and e refer to Eqs. (3.19), (3.20), (3.22) and (3.23), (3.24) and (3.25), and (3.27) and (3.31), respectively. The asterisk (*) on ^{6}Li refers to the three-body correlation parameters used with the modified wave function.

Nucleus	$q^c_{1\text{-}2}(sss)^a$	$q^c_{1\text{-}2}(ssp)^a$	$q^c_{1\text{-}2}(spp)^a$	$q^{p\ b}_{1\text{-}2}$	$q^{ls\ c}_{1\text{-}3}$	$q^{\tau\ d}_{1\text{-}4}$	$\delta_{1\text{-}3}{}^e$	$r_s{}^e$
^{3}H	0.20	–	–	0.16	−0.013	−0.013	−0.00025	0.70
	0.85			0.05	0.12	0.015	−0.00040	
					0.85	1.200	−0.00060	
						0.350		
^{4}He	0.18	–	–	0.17	−0.12	−0.012	−0.00018	0.70
	0.88			0.05	0.12	0.0015	−0.00048	
					0.86	1.200	−0.00053	
						0.360		
^{6}Li	0.184	0.051	0.672	0.16	−0.05	−0.005	−0.00021	0.66
	0.856	0.880	0.381	0.05	0.12	0.015	−0.00040	
					0.85	1.200	−0.00041	
						0.350		
^{6}Li*							−0.000375	0.72
							−0.000100	
							−0.000500	

TABLE VI. Variational parameters for ^{4}He corresponding to modifications in the wave function. The healing distance r_d^x is in femtometers.

Corr.$\backslash n$	1	2	3	4	5	6	7	r_d^x
a_n^c	0.12452×10^{-2}	-0.29732×10^{-2}	-0.86371×10^{-2}	-0.38410×10^{-2}	-0.38796×10^{-2}	-0.47343×10^{-3}	-0.11390×10^{-2}	8.706
a_n^τ	-0.43984×10^{-2}	0.29679×10^{-2}	0.22546×10^{-2}	0.90877×10^{-3}	0.20779×10^{-2}	-0.84671×10^{-3}	0.10404×10^{-2}	7.398
a_n^σ	-0.23762×10^{-2}	0.65719×10^{-2}	0.19283×10^{-2}	0.23395×10^{-2}	0.30933×10^{-2}	-0.42067×10^{-3}	0.17577×10^{-2}	7.113
$a_n^{\sigma\tau}$	0.32188×10^{-3}	-0.82182×10^{-3}	-0.26743×10^{-3}	0.57667×10^{-3}	0.68396×10^{-3}	0.18796×10^{-3}	0.55954×10^{-3}	6.446
a_n^t	0.66134×10^{-4}	-0.71330×10^{-3}	-0.12813×10^{-2}	-0.26590×10^{-2}	-0.15165×10^{-2}	-0.13263×10^{-2}	-0.88126×10^{-3}	6.420
$a_n^{t\tau}$	-0.63054×10^{-3}	-0.16978×10^{-2}	0.33158×10^{-2}	0.12607×10^{-2}	-0.35203×10^{-3}	0.47092×10^{-4}	0.26309×10^{-3}	9.955
a_n^b	-0.26177×10^{-2}	-0.42627×10^{-2}	-0.31190×10^{-2}	-0.28810×10^{-2}	-0.30691×10^{-2}	-0.13588×10^{-2}	-0.12405×10^{-2}	5.557
$a_n^{b\tau}$	-0.33149×10^{-3}	0.37375×10^{-3}	0.43159×10^{-3}	-0.13868×10^{-3}	-0.30010×10^{-3}	-0.31242×10^{-3}	-0.85590×10^{-3}	5.000
a_n^h	-0.11971×10^{-1}	-0.14902×10^{-1}	-0.56484×10^{-2}	-0.35629×10^{-2}	-0.21307×10^{-2}	-0.14296×10^{-2}	-0.64099×10^{-3}	3.872
a_n^g	0.10722	0.88876×10^{-1}	0.54161×10^{-1}	-0.67214×10^{-2}	-0.25431×10^{-1}	-0.21486×10^{-1}	-0.72686×10^{-2}	2.949
a_n^{aT}	0.66963	-0.11947×10^{-1}	−0.88402	−0.17112	0.43091×10^{-1}	0.13386	0.17782	4.114
a_n^{aY}	0.48653	−0.62868	−0.36267	0.39732	0.34618	0.68349×10^{-1}	-0.63176×10^{-1}	3.854
a_n^{cT}	3.7494	11.099	8.9406	2.1909	−1.8355	−1.3509	−0.90447	2.322
a_n^{cY}	5.7041	−2.6631	2.9193	−0.39743	−0.29865	0.22578	−0.55806	5.469
a_n^R	4.9140	−0.25399	−0.41839	−0.57731	−0.19738	0.23982	−0.11791	2.993

Eq. (2.6). The parameter values in Tables VI and VII are not unique, in the sense that it is possible to find other sets of parameters with essentially the same energies and variances but with somewhat different energy breakup. This problem is related to the occurrence of a flat energy minima, perhaps several of them, in the multidimensional parameter space. Since we minimize a combination of energy and variance, it is indeed difficult to ascertain that we have reached the lowest energy. Probably, an optimization along the lines of what was done in Ref. [12] will be more suitable, but this requires considerable effort both computationally as well as from a programming point of view.

It is instructive to know how the energy can be optimized or lowered with respect to modifications in various correlations. We have studied this by generating a random walk with the best set of our parameters (Tables VI and VII) and switching off the modifications one at a time for each correlation and then calculating the change in the energy, ΔE, for the same random walk. The results are displayed in Table VIII for ^{4}He and ^{6}Li. We also give the variance σ for each such case. The first column lists the various correlations. The row for a specific correlation, for example f_c, gives the change ΔE and the new σ by keeping all the optimized changes in each correlation except for f_c, for which we use the unmodified values corresponding to $K = 0$. It is evident from the table that modifications in f_6 correlations play a role for both the nuclei, but much more significantly in ^{6}Li, where ΔE for $u_{\sigma\tau}$, u_t, $u_{t\tau}$, and f_c are, respectively, 1.68, 0.62, 0.51, and 0.49 MeV. Table VIII also displays how sensitive the energies and variances are to modifications in various correlations. Does this imply that modifying only one correlation, for example $u_{\sigma\tau}$, can lower the energy of ^{6}Li close to ≈ -29.7 MeV? The answer is no. What is important is the totality of all the changes in the f_6 correlations. We shall elaborate on this a little later. Such large values of ΔE may then bring large changes in the corresponding correlations, which may also depend on how sensitive a particular correlation is to the energy. In Fig. 4, we display all the f_6 correlations. The solid and dashed curves refer to ^{6}Li and the dashed-dotted and dashed-double-dotted curves refer to ^{4}He. The solid and dashed-dotted (dashed and dashed-double-dotted) curves refer to modified (unmodified) correlations. It may be seen that the dashed and dashed-double-dotted curves more or less coincide, implying that the unmodified f_6 correlations are almost the same for both systems. This is by design. Intuitively, one may expect them to be close as the difference between the binding energies of ^{6}Li and ^{4}He is small. However, from Fig. 4 we see that the modified correlations in ^{6}Li and ^{4}He (the solid and dashed-dot curves) differ from each other. This difference is represented by the dotted curve after multiplying the differences by f_c for u_τ to $u_{t\tau}$ [Figs. 4(b)–4(f)]. It is seen that the differences are appreciable for $u_{\sigma\tau}$ and u_t. We discuss in the following the implications of these results.

The experimental difference in the binding energies of ^{4}He and ^{6}Li is around 3.7 MeV. Thus the p-shell nucleons in ^{6}Li interact weakly with the ^{4}He core. Such a weak binding can change the tightly bound ^{4}He core only by a small amount. This is also evident from the studies in hypernuclei [5,27,28], where it has been shown that in $^5_\Lambda$He, the energy of the ^{4}He core (called the rearrangement or core-polarization energy E_R) changes by $\approx$0.39(6) MeV, corresponding to a Λ binding of 3.1 MeV. The corresponding changes in the wave functions are also very small, in contrast to the findings of the present study. This may give rise to a false conclusion that the rearrangement energy of the ^{4}He core in ^{6}Li may be large. However, we demonstrate that this is not the case.

We obtain E_R from

$$E_R \approx \frac{\langle\Psi_m|H|\Psi_m\rangle}{\langle\Psi_m|\Psi_m\rangle} - \frac{\langle\Psi|H|\Psi\rangle}{\langle\Psi|\Psi\rangle} \equiv E_m - E, \qquad (4.6)$$

where Ψ_m is the core nucleus wave function of ^{4}He modified by the presence of extra p-shell nucleons, and Ψ is the optimized wave function of the isolated core nucleus. E_m and E are, respectively, the expectation values of the Hamiltonian with Ψ_m and Ψ. This estimate of E_R is an approximation to the rigorous definition given in Ref. [28] but is much simpler to implement and at the same time quite accurate. When we substitute for Ψ_m the optimized part of the two- and three-body correlations of the ^{6}Li wave function in Eq. (3.6), we obtain $E_m = -27.68(3)$ MeV and $E_R = 0.22(3)$ MeV. This demonstrates that the rearrangement energy is small and the

TABLE VII. Variational parameters for ^{6}Li corresponding to modifications in the wave function. The healing distance r_d^x is in femtometers. $a_n^p(1–3)$ and $a_n^{pp}(1–3)$ correspond to $\phi_p(1–3)$ and $f_{pp}(1–3)$, respectively, for different combinations of $LS[n]$.

Corr.\n	1	2	3	4	5	6	7	8	9	10	11	r_d^x
a_n^c	0.36267×10^{-2}	-0.26657×10^{-1}	-0.63862×10^{-2}	-0.57766×10^{-2}	-0.21549×10^{-2}	-0.19193×10^{-2}	-0.10756×10^{-2}	-0.78767×10^{-3}	-0.15421×10^{-2}	-0.77246×10^{-4}	-0.54157×10^{-3}	6.881
a_n^τ	-0.24012×10^{-1}	-0.97402×10^{-3}	0.14738×10^{-1}	-0.15569×10^{-2}	0.36168×10^{-2}	-0.63818×10^{-3}	0.65537×10^{-2}	-0.57087×10^{-3}	0.31032×10^{-2}	0.26397×10^{-2}	0.11915×10^{-2}	21.522
a_n^σ	-0.12500×10^{-1}	-0.19901×10^{-2}	0.57443×10^{-2}	0.70963×10^{-3}	0.41945×10^{-2}	-0.98097×10^{-3}	0.14878×10^{-2}	-0.39327×10^{-3}	0.29299×10^{-3}	0.17019×10^{-3}	0.24866×10^{-3}	10.858
$a_n^{\sigma\tau}$	-0.13215×10^{-1}	-0.20010×10^{-1}	-0.54795×10^{-2}	-0.31993×10^{-2}	-0.11350×10^{-2}	-0.27123×10^{-3}	0.42576×10^{-3}	0.97098×10^{-4}	0.34497×10^{-3}	0.43317×10^{-3}	0.22097×10^{-3}	10.062
a_n^t	0.20044×10^{-2}	-0.54793×10^{-2}	-0.48923×10^{-3}	-0.27165×10^{-2}	-0.35150×10^{-3}	-0.15182×10^{-2}	-0.59053×10^{-3}	-0.92509×10^{-3}	-0.64188×10^{-3}	-0.36447×10^{-3}	-0.25552×10^{-3}	10.266
$a_n^{t\tau}$	-0.41534×10^{-2}	-0.60388×10^{-2}	0.76703×10^{-3}	-0.12024×10^{-2}	0.10566×10^{-2}	-0.34302×10^{-3}	0.61984×10^{-3}	-0.50788×10^{-4}	0.42610×10^{-3}	0.17127×10^{-4}	0.15769×10^{-3}	10.415
a_n^b	-0.72366×10^{-3}	-0.82988×10^{-3}	-0.82580×10^{-3}	-0.93086×10^{-3}	-0.11156×10^{-2}	-0.11102×10^{-2}	-0.10722×10^{-2}	-0.80041×10^{-3}	-0.52775×10^{-3}	-0.23009×10^{-3}	-0.53580×10^{-4}	7.971
$a_n^{b\tau}$	0.16270×10^{-2}	0.13058×10^{-2}	0.77108×10^{-3}	0.60229×10^{-4}	-0.40296×10^{-3}	-0.48431×10^{-3}	-0.36971×10^{-3}	-0.16075×10^{-3}	-0.70999×10^{-4}	-0.79576×10^{-4}	-0.90403×10^{-4}	−4.880
a_n^{sp}	0.44181×10^{-2}	0.11889×10^{-1}	0.69506×10^{-2}	0.10748×10^{-1}	0.63120×10^{-2}	0.37749×10^{-2}	0.15112×10^{-2}	0.10974×10^{-2}	0.37905×10^{-3}	0.54164×10^{-3}	0.86655×10^{-3}	8.970
$a_n^p(1)$	-0.37399×10^{-2}	-0.72028×10^{-2}	0.44877×10^{-3}	0.15842×10^{-2}	0.84495×10^{-3}	0.25574×10^{-3}	0.26597×10^{-3}	0.25695×10^{-3}	0.65964×10^{-3}	0.43017×10^{-3}	0.43980×10^{-3}	14.460
$a_n^p(2)$	-0.93472×10^{-3}	-0.92055×10^{-2}	-0.88730×10^{-2}	-0.70794×10^{-2}	-0.11060×10^{-2}	0.26069×10^{-2}	0.55168×10^{-3}	0.66705×10^{-3}	-0.16231×10^{-3}	0.64599×10^{-3}	-0.67672×10^{-3}	9.738
$a_n^p(3)$	0.33533×10^{-2}	0.23563×10^{-1}	0.12940×10^{-1}	0.53124×10^{-2}	-0.13273×10^{-2}	-0.44210×10^{-2}	-0.30700×10^{-2}	-0.49548×10^{-2}	-0.28161×10^{-2}	-0.15597×10^{-2}	-0.11541×10^{-2}	13.219
$a_n^{pp}(1)$	-0.86525×10^{-2}	0.27054×10^{-1}	-0.80608×10^{-2}	0.11950×10^{-1}	0.38384×10^{-2}	0.31643×10^{-2}	0.82486×10^{-2}	0.40579×10^{-2}	0.27944×10^{-2}	0.38183×10^{-2}	-0.24575×10^{-3}	18.281
$a_n^{pp}(2)$	0.88230×10^{-1}	0.10695	-0.74458×10^{-2}	-0.83792×10^{-2}	-0.14158×10^{-1}	-0.30050×10^{-2}	-0.12833×10^{-1}	-0.44826×10^{-3}	-0.45639×10^{-2}	-0.35540×10^{-2}	-0.45293×10^{-3}	11.153
$a_n^{pp}(3)$	0.0	0.0	0.0	0.0	0.0	0.0	0.0	0.0	0.0	0.0	0.0	–
a_n^h	-0.91997×10^{-4}	-0.79732×10^{-2}	-0.16232×10^{-3}	0.19008×10^{-2}	0.18305×10^{-2}	0.68484×10^{-3}	0.47071×10^{-3}	-0.29556×10^{-4}	0.53624×10^{-4}	-0.10640×10^{-4}	0.21449×10^{-5}	4.959
a_n^g	0.82296	0.24481	-0.66051×10^{-1}	-0.55466×10^{-1}	-0.47134×10^{-2}	0.85527×10^{-2}	-0.26936×10^{-2}	0.00000	0.00000	0.00000	0.00000	1.480
a_n^{aT}	−0.94429	−0.92623	0.13228	0.36117	0.47688	0.33309	0.24896	0.94770×10^{-1}	0.27942×10^{-1}	-0.64787×10^{-1}	-0.43195×10^{-2}	4.727
a_n^{aY}	0.00000	−1.1931	−0.12862	−0.47552	−0.57287	−0.23710	−0.11543	0.10707×10^{-1}	0.85791×10^{-1}	0.00000	0.13212	2.600
a_n^{cT}	1.4293	−2.5603	−3.8987	−2.1304	−1.5410	−1.5410	0.24041	0.00000	0.00000	0.00000	0.00000	2.371
a_n^{cY}	1.8919	−2.6676	-7.0117×10^{-1}	−0.67757	−0.60574	−0.34252	0.14531	0.18370	-0.96326×10^{-1}	−0.10210	0.89852×10^{-1}	2.758
a_n^R	7.0237	6.0773	5.4620	0.26604	−1.8071	−1.6262	−0.74026	−0.76745	−0.42521	−0.46251	−0.16605	4.539

TABLE VIII. ΔE and σ due to switching off the variational correlations one at a time. h and g refer to Eqs. (3.22) and (3.23), respectively. $Y_\pi\{\ \}$, $T_\pi\{\ \}$, $Y_\pi[\ ]$, and $T_\pi[\ ]$ are the Yukawa and tensor radial shapes for the anticommutator $\{\ \}$ and commutator $[\ ]$ terms, which refer to Eq. (3.28). T_π^2 refers to Eq. (3.31).

Switching off the Modifications in	^{4}He		^{6}Li	
	ΔE (MeV)	σ (MeV)	ΔE (MeV)	σ (MeV)
None	0.0	0.0198	0.0	0.0273
f_c	0.038(13)	0.0248	0.491(29)	0.0427
u_τ	0.020(5)	0.0208	0.328(14)	0.0325
u_σ	0.062(7)	0.0219	0.175(4)	0.0283
$u_{\sigma\tau}$	0.032(6)	0.0208	1.677(29)	0.0360
u_t	0.080(7)	0.0213	0.622(8)	0.0279
$u_{t\tau}$	0.096(4)	0.0201	0.510(10)	0.0280
u_b	0.012(1)	0.0198	0.010(0)	0.0273
$u_{b\tau}$	0.014(1)	0.0198	0.058(1)	0.0270
f_{sp}	–	–	0.038(1)	0.0078
$f_{pp}(1)$	–	–	0.114(8)	0.0280
$f_{pp}(2)$	–	–	0.017(2)	0.0273
$f_{pp}(3)$	–	–	0.000(0)	0.0000
$\phi_p(1)$	–	–	0.214(10)	0.0297
$\phi_p(2)$	–	–	0.003(2)	0.0274
$\phi_p(3)$	–	–	0.027(1)	0.0273
h	0.017(1)	0.0199	0.088(2)	0.0275
g	0.0180(1)	0.0198	0.015(1)	0.0272
$Y_\pi\{\ \}$	0.012(3)	0.0204	0.073(6)	0.0276
$T_\pi\{\ \}$	0.019(6)	0.0208	0.135(9)	0.0277
T_π^2	0.057(22)	0.0294	0.007(9)	0.0292
$Y_\pi[\ ]$	0.094(9)	0.0226	0.028(8)	0.0278
$T_\pi[\ ]$	0.034(10)	0.0229	0.088(6)	0.0297

extra p-shell nucleons in ^{6}Li modify the ^{4}He core only slightly. This is consistent with the studies in hypernuclei mentioned earlier. This result is also consistent with the estimates of Ref. [8], where it is found that the ^{4}He cores in ^{6,8}He nuclei are excited by $\approx$0.08 and 0.35 MeV, respectively.

The small value of E_R and at the same time large differences between the two correlations (solid and dashed-dot curves of Fig. 4) can be reconciled in the following manner. It is related to having different correlations in the even and odd states in ^{6}Li since the interactions between the two states are different. In addition, there are different constraints and symmetries associated with angular momentum values. This difference is also accentuated by the greater number of sp pairs (eight) as compared to ss pairs (six) in ^{6}Li. The even-state correlations are perhaps very close to the ^{4}He correlations. Thus, most of the difference between the solid and dashed-dot curves of Fig. 4 may arise from the odd-state correlations in ^{6}Li, which are different from the even-state correlations. Every correlation can be broken into even and odd components. We consider here a specific operator

$$u_\tau \vec{\tau}_i \cdot \vec{\tau}_j = \left[u_{\tau e}\tfrac{1}{2}(1+P_x) + u_{\tau o}\tfrac{1}{2}(1-P_x)\right]\vec{\tau}_i \cdot \vec{\tau}_j, \quad (4.7)$$

where $u_{\tau e}$ and $u_{\tau o}$ refer to even and odd states, respectively, and P_x is the Majorana space exchange operator, which for an antisymmetric wave function is $-P_\sigma P_\tau$, where P_σ and P_τ are the spin and isospin exchange operators, respectively. Simple algebra then gives

$$\begin{aligned} u_\tau \vec{\tau}_i \cdot \vec{\tau}_j = {} & \tfrac{3}{8}(u_{\tau o} - u_{\tau e}) + \tfrac{1}{8}(5u_{\tau e} + 3u_{\tau o})\,\vec{\tau}_i \cdot \vec{\tau}_j \\ & + \tfrac{3}{8}(u_{\tau e} - u_{\tau o})\,\vec{\sigma}_i \cdot \vec{\sigma}_j + \tfrac{1}{8}(u_{\tau e} - u_{\tau o}) \\ & \times (\vec{\sigma}_i \cdot \vec{\sigma}_j)(\vec{\tau}_i \cdot \vec{\tau}_j). \end{aligned} \quad (4.8)$$

The first term on the right-hand side can be grouped with f_c, the third with u_σ, and the last with $u_{\sigma\tau}$. Thus all the correlation modify others if even- and odd-state correlations differ. Similar considerations hold for tensor and spin-orbit correlations. This is the reason why f_c is modified in ^{6}Li, though a separate central correlation, f_{sp}, has been incorporated between the s- and p-shell nucleons. Our optimization scheme takes care of the possibility of incorporating the even-odd state correlations in a convenient way. This also explains, as mentioned earlier, that it is the totality of modification in all the correlations, not a particular one, that is responsible in reducing the energy of ^{6}Li by $\approx$1.7 MeV. Though we have not explicitly separated the even and odd components, we believe that the even-state components of ^{6}Li should be close to that of ^{4}He, which leads to a small value of E_R as it should.

The modifications in three-body correlations do not play such a great role as they do the f_6 in ^{6}Li. However, as is evident from Table VIII, their role cannot be ignored.

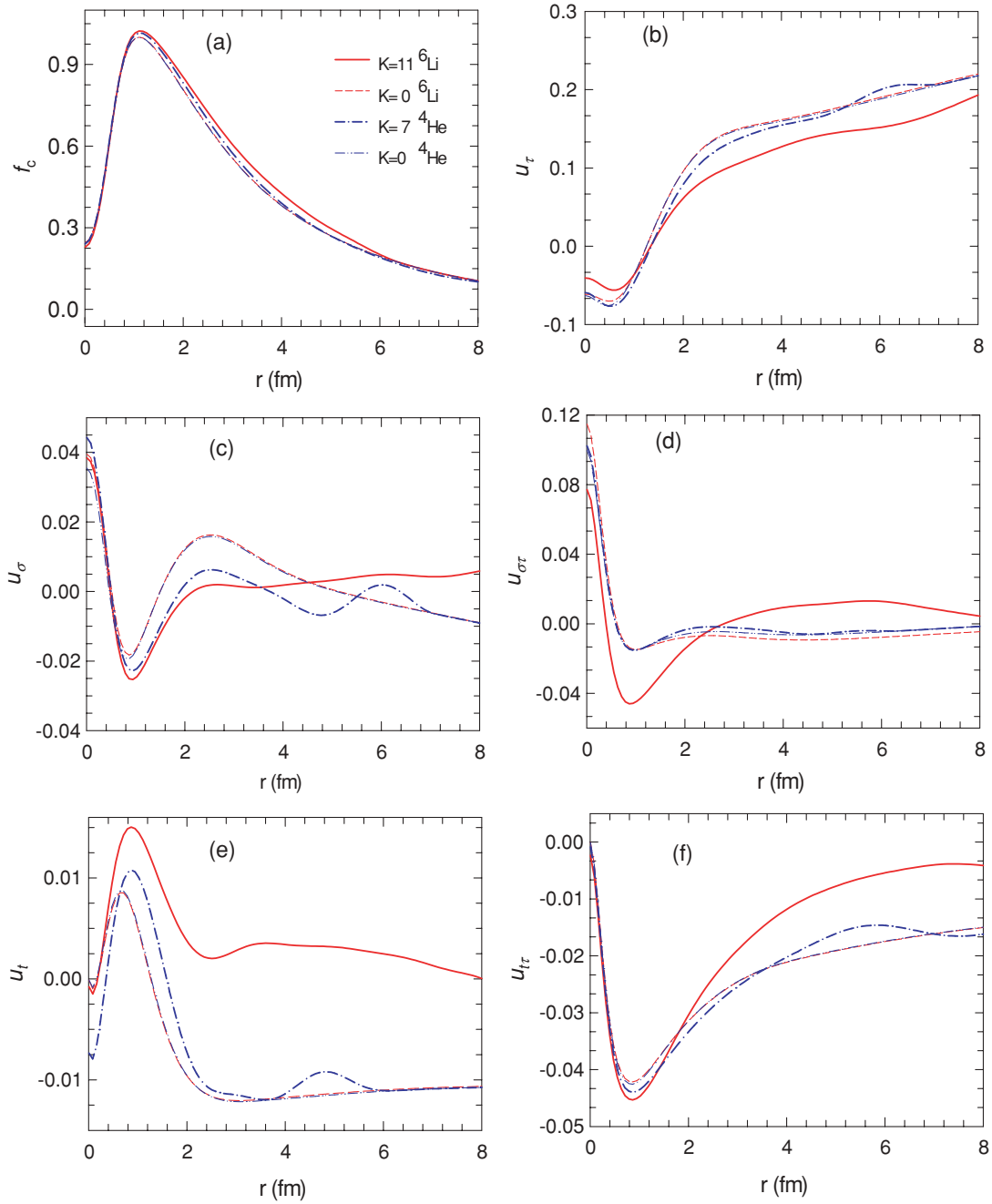

FIG. 4. (Color) The f_6 correlations in ^{4}He and ^{6}Li as a function of internucleon distance. The legends for u_τ to $u_{t\tau}$ are same as for f_c.

We notice a few wiggles in ^{4}He correlations in u_σ, u_t, and $u_{t\tau}$. The ^{6}Li correlations do not have pronounced wiggles but still have some wavy character for large values of r. We do not know the reasons for these. It is possible that the energies are insensitive to these wiggles, which result from *overparametrization* of the correlations. We have, however, not looked into it.

The large number of new variational parameters introduced may seem awkward, but we cannot undermine their importance. They do demonstrate that better VMC energies can be achieved if improved correlation shapes are employed. It would be extremely useful to search for suitable correlation functions with fewer parameters.

We believe we have stretched the PANDC correlations to their limits, though there is scope for considerable modifications in the wave functions and energies for all the nuclei studied. However, these can be realized only with new correlation structures and shapes and preferably with fewer parameters. This will be the subject of a future study. It is likely that the missing correlations in ^{6}Li that will bring the results into conformity or close to GFMC values may have the same origin as in the s-shell nuclei.

V. CONCLUSIONS

We have presented an error analysis of the variational many-body wave functions that is based on somewhat general considerations. Improvements in the wave functions are proposed to minimize the errors. These are implemented for central and operatorial two- and three-body correlations, which lead to improvement in the energies and reduction in the statistical Monte Carlo variance. A significant reduction in the ^{6}Li energy is obtained, but still this nucleus is unbound with respect to breakup into ^{4}He and a deuteron cluster, though now with less than 0.5 MeV. We have given the details of the wave functions so that the results can be reproduced with a little effort and can be used in other calculations. We have discussed in detail the manifestation of odd-state correlations in ^{6}Li and its implications.

It is hoped that similar improvements can be obtained for other p-shell nuclei. The present development paves the way for carrying out calculations for heavy nuclei using the cluster variational Monte Carlo technique in a more reliable way. Also improvements on similar lines can be implemented for helium liquids and nuclear matter within the variational framework. Indeed, application of the proposed technique to hypernuclei will be of great importance in deciphering information on the baryon-baryon interaction in the strange sector [5,6,28,29] and these wave functions will be useful in GFMC and diffusion Monte Carlo calculations [30].

ACKNOWLEDGMENTS

QNU is especially grateful to Robert B. Wiringa for providing the VMC code for s- and p-shell nuclei. He thanks him and Steven C. Pieper for supporting his visits to Argonne National Laboratory. Both QNU and GR are indebted to Richard F. Casten for allowing them to use the facilities of the Wright Nuclear Structure Laboratory at Yale University, where part of this work was carried out. The work related to the central potential was carried out at the JMI (New Delhi) Physics Department computing facility, for which we gratefully acknowledge Tabish Qureshi for help in computing. QNU and KA acknowledge the Rocks-Clusters project and its core team, Greg Bruno, Mason Katz, Philip Papadopoulos, Anoop Rajendra, and many others on npaci-rocks-discussion@sdsc.edu, namely, Cole Brand, Gustavo Correa, Gerry Creager, Jon Forrest, Scott L. Hamilton, Mike Hanby, Ian Kaufman, Olivier de Kermoysan, Vlad Manea, and Divi Venkateshwarlu. It is with the help of these people that we could successfully build a cluster with a rudimentary knowledge of Linux. Most of the calculations were performed on this cluster. The Rocks-Clusters project is supported by NSF Grant No. OCI-0721623.

[1] R. B. Wiringa and R. Schiavilla, Phys. Rev. Lett. **81**, 4317 (1998).
[2] L. Lapikás, J. Wesseling, and R. B. Wiringa, Phys. Rev. Lett. **82**, 4404 (1999).
[3] A. H. Wuosmaa *et al.*, Phys. Rev. Lett. **94**, 082502 (2005).
[4] K. M. Nollett, Phys. Rev. C **63**, 054002 (2001).
[5] Q. N. Usmani, A. R. Bodmer, and B. Sharma, Phys. Rev. C **70**, 061001(R) (2004).
[6] M. Shoeb and Sonika, Phys. Rev. C **79**, 054321 (2009).
[7] J. Carlson and R. Schiavilla, Rev. Mod. Phys. **70**, 743 (1998), and references therein.
[8] S. C. Pieper and R. B. Wiringa, Annu. Rev. Part. Sci. **51**, 53 (2001), and references therein.
[9] R. B. Wiringa, La Physique au Canada **64**, 67 (2008).
[10] S. C. Pieper, Nucl. Phys. **A751**, 516c (2005).
[11] M. Pervin, S. C. Pieper, and R. B. Wiringa, Phys. Rev. C **76**, 064319 (2007); K. M. Nollett, S. C. Pieper, and R. B. Wiringa, Phys. Rev. Lett. **99**, 022502 (2007); R. Schiavilla, R. B. Wiringa, S. C. Pieper, and J. Carlson, *ibid.* **98**, 132501 (2007); V. V. Flambaum and R. B. Wiringa, Phys. Rev. C **76**, 054002 (2007); L. E. Marcucci, K. M. Nollett, R. Schiavilla, and R. B. Wiringa, Nucl. Phys. **A777**, 111 (2006).
[12] C. J. Umrigar and Claudia Filippi, Phys. Rev. Lett. **94**, 150201 (2005), and references therein.
[13] R. B. Wiringa, V. G. J. Stoks, and R. Schiavilla, Phys. Rev. C **51**, 38 (1995).
[14] B. S. Pudliner, V. R. Pandharipande, J. Carlson, and R. B. Wiringa, Phys. Rev. Lett. **74**, 4396 (1995).
[15] D. R. Thompson, M. LeMere, and Y. C. Tang, Nucl. Phys. **A286**, 53 (1977); I. Reichstein and Y. C. Tang, *ibid.* **A158**, 529 (1970).
[16] R. A. Malfliet and J. A. Tjon, Nucl. Phys. **A127**, 161 (1969).
[17] K. Varga and Y. Suzuki, Phys. Rev. C **52**, 2885 (1995).
[18] V. R. Pandharipande, Nucl. Phys. **A174**, 641 (1971).
[19] J. Lomnitz Adler and V. R. Pandharipande, Nucl. Phys. **A342**, 404 (1980); J. Lomnitz Adler, V. R. Pandharipande, and R. A. Smith, *ibid.* **A361**, 399 (1981).
[20] J. Carlson, V. R. Pandharipande, and R. B. Wiringa, Nucl. Phys. **A401**, 59 (1983).
[21] R. B. Wiringa, Phys. Rev. C **43**, 1585 (1991).
[22] A. Arriaga, V. R. Pandharipande, and R. B. Wiringa, Phys. Rev. C **52**, 2362 (1995).
[23] A. A. Usmani, S. C. Pieper, and Q. N. Usmani, Phys. Rev. C **51**, 2347 (1995); S. C. Pieper, R. B. Wiringa, and V. R. Pandharipande, *ibid.* **46**, 1741 (1992); M. L. Ristig and J. W. Clark, Nucl. Phys. **A199**, 351 (1973).
[24] S. Cohen and D. Kurath, Nucl. Phys. **73**, 1 (1965).
[25] R. B. Wiringa (private communication).
[26] J. Fujita and H. Miyazawa, Prog. Theor. Phys. **17**, 360 (1957).
[27] Q. N. Usmani, A. R. Bodmer, and Z. Sauli, Phys. Rev. C **77**, 034312 (2008).
[28] A. R. Bodmer, S. Murali, and Q. N. Usmani, Nucl. Phys. **A609**, 326 (1996).
[29] R. Sinha, Q. N. Usmani, and B. M. Taib, Phys. Rev. C **66**, 024006 (2002); R. Sinha and Q. N. Usmani, Nucl. Phys. **A684**, 586c (2001); Q. N. Usmani and A. R. Bodmer, *ibid.* **A639**, 147c (1998); Phys. Rev. C **60**, 055215 (1999).
[30] S. Gandolfi, F. Pederiva, S. Fantoni, and K. E. Schmidt, Phys. Rev. Lett. **98**, 102503 (2005); **99**, 022507 (2007); S. Gandolfi, A. Yu. Illarionov, K. E. Schmidt, F. Pederiva, and S. Fantoni, arXiv:0903.2610 (March 2009), and references therein.